

# Optical band gap and FT-IR studies on $\text{Cu}^{2+}$ doped $20\text{ZnO} + x\text{Li}_2\text{O} + (30-x)\text{Na}_2\text{O} + 50\text{B}_2\text{O}_3$ glasses

T. RAGHAVENDRA RAO<sup>a,\*</sup>, CH. VENKATA REDDY<sup>a,b</sup>, U. S. UDAYCHANDRAN THAMPY<sup>a,c</sup>,  
CH. RAMA KRISHNA<sup>a</sup>, Y. P. REDDY<sup>d</sup>, P. SAMBASIVA RAO<sup>e</sup>, R. V. S. S. N. RAVIKUMAR<sup>a</sup>

<sup>a</sup>Department of Physics, Acharya Nagarjuna University, Nagarjuna Nagar-522 510, India

<sup>b</sup>Department of Physics, K.L. University, Guntur-522 502, India

<sup>c</sup>Department of Physics, University of Kerala, Kariavattom Campus, Thiruvananthapuram, Kerala-695581, India

<sup>d</sup>Co-ordinator, Physical Sciences, Sri Padmavati Mahila Viswavidyalayam, Tirupati -517 502, India

<sup>e</sup>Department of Chemistry, Pondicherry University, Pondicherry- 605 014, India

The spectral studies on  $20\text{ZnO}+x\text{Li}_2\text{O}+(30-x)\text{Na}_2\text{O}+50\text{B}_2\text{O}_3$  ( $5 \leq x \leq 25$ ) doped with 0.1 mol% of paramagnetic CuO impurity are carried out. XRD patterns of powder glass samples confirm the amorphous nature. Urbach energies are shown the structural stability of the systems. The optical band gap energies varies non-linearly within the range of 3.818 – 4.073 eV for direct and 3.770 – 4.024 eV for indirect transitions with the increase of  $\text{Li}_2\text{O}$  content. The FT-IR spectral studies show that the glass systems contain  $\text{BO}_3$  and  $\text{BO}_4$  units in disordered manner. The structural changes have been observed with alkali contents of the systems. It is observed that the system is more stable at  $x = 20$  mol%. Mixed Alkali Effect phenomenon has been explained in the glass host.

(Received July 24, 2012; accepted February 20, 2013)

**Keywords:** Mixed alkali zinc borate glass, Absorption edge, Optical band gap, Urbach energy and FT-IR

## 1. Introduction

The transition metal ions doped alkali borate glasses have many technological applications due to their electrical and optical properties. Borate glasses are used as electro-optic switches, electro-optic modulators, solid state laser materials, non-linear optical parametric converters, insulating materials and cathode materials for batteries [1-5]. Zinc containing glasses have wide band gap, low melting point and have been widely used as a good sintering agents [6-9]. When one alkali is progressively substituted for another, many physical properties of oxide glasses show non-linear behavior as a function of alkali content. Mixed Alkali Effect (MAE) is one of the outstanding problems and is a poorly understood phenomenon in glass science [10-21]. The majority of existing literature on MAE is based on dynamic studies. The structure of pure vitreous  $\text{B}_2\text{O}_3$  consists of a random network of boroxyl rings and  $\text{BO}_3$  triangles connected by B–O–B linkage [22]. The addition of alkali oxides modifies the boroxyl rings; complex borate groups with one or two four co-ordinate borate atoms are formed [23]. MAE in phosphate glasses has been reported in which CuO is used as a paramagnetic probe [24-26]. Recently authors have been published MAE of different transition metal ions doped Alkali Zinc Borate Glasses and

ascertained the site symmetry, bonding nature and physical parameters [27-33]. The aim of the present study is to examine the MAE in copper doped  $20\text{ZnO} + x\text{Li}_2\text{O} + (30-x)\text{Na}_2\text{O} + 50\text{B}_2\text{O}_3$  ( $5 \leq x \leq 25$ ) glasses using spectroscopic techniques like powder XRD, optical absorption and FT-IR studies to get a comprehensive view.

## 2. Experimental

### 2.1. Preparation of glasses

Analar grade ZnO (99.9%),  $\text{B}_2\text{O}_3$  (99.9%),  $\text{Li}_2\text{CO}_3$  (99.9%) and  $\text{Na}_2\text{CO}_3$  (99.9%) are taken as starting materials for the present study. The host glass composition is taken in the ratio as mentioned in Table 1. For transition metal doping, 0.1 mol% of copper oxide is added to starting materials. These mixtures are sintered at 750 K and melted in an electric furnace in silica crucible around 1250 K for nearly 1h. The melt is then quenched at room temperature in air to form a glass. The glasses so formed are annealed at 700 K for 1h to relieve the structural stress.

Table 1. Composition of glasses studied in the present work.

Glass System	Glass Chemical Composition	Prepared temp.
ZLNB1	19.9 ZnO + 5 Li <sub>2</sub> O + 25 Na <sub>2</sub> O+ 50 B <sub>2</sub> O <sub>3</sub> + 0.1 CuO	1175 K
ZLNB2	19.9 ZnO + 10 Li <sub>2</sub> O + 20 Na <sub>2</sub> O+ 50 B <sub>2</sub> O <sub>3</sub> + 0.1 CuO	1188 K
ZLNB3	19.9 ZnO + 15 Li <sub>2</sub> O + 15 Na <sub>2</sub> O+ 50 B <sub>2</sub> O <sub>3</sub> + 0.1 CuO	1213 K
ZLNB4	19.9 ZnO + 20 Li <sub>2</sub> O + 10 Na <sub>2</sub> O+ 50 B <sub>2</sub> O <sub>3</sub> + 0.1 CuO	1223 K
ZLNB5	19.9 ZnO + 25 Li <sub>2</sub> O + 5 Na <sub>2</sub> O+ 50 B <sub>2</sub> O <sub>3</sub> + 0.1 CuO	1223 K

## 2.2. Measurements

The X-ray diffraction patterns of powder glass samples are recorded on PANalytical XpertProdiffractometer with copper K $\alpha$  radiation. The optical absorption spectra of polished glass samples are recorded on JASCO V670 spectrophotometer in the region of 200-1400 nm. The optical band gap energies for direct and indirect transitions and Urbach energies of all the samples are calculated. FT-IR spectra are recorded using KBr pellets on Thermo Nicolet 6700 FT-IR spectrophotometer in the region 400-4000 cm<sup>-1</sup>.

## 3. Results and discussions

### 3.1. Powder X-ray diffraction studies

The x-ray diffraction pattern consists of a few broad diffuse haloes rather than sharp rings which is a sign of amorphous material. All the prepared glass samples confirm the amorphous nature. Fig. 1 shows the typical x-ray diffraction patterns for undoped and copper doped glasses.

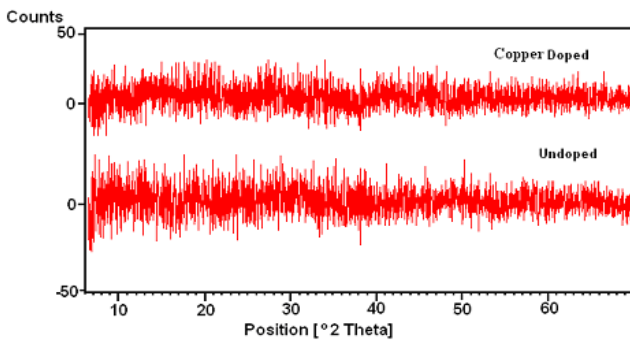


Fig. 1. Powder X-ray diffraction patterns of Cu<sup>2+</sup> doped and undoped ZLNB glasses.

### 3.2. Optical band gap and Urbach energy studies

The study of the fundamental absorption edge in the UV region is a useful method for the investigation of optical transitions, electronic band structure in crystalline and non-crystalline materials. There are two types of

optical transitions that can occur at the fundamental absorption edge of crystalline and non-crystalline materials. They are direct and indirect transitions. In both the cases, electromagnetic waves interact with the electrons in the valence band, which are raised across the fundamental gap to the conduction band. In glasses, the conduction band is influenced by the glass forming anions; the cations play an indirect but significant role. Classical optical transmission on the bulk samples with the thickness varying in the region 0.5 – 4  $\mu$ m prepared by a glass blowing was measured [34]. Davis and Mott [35] gave the following forms of absorption co-efficient  $\alpha(\nu)$  as a function of photon energy for direct and indirect transitions. For direct transitions,

$$\alpha(\nu) = B(h\nu - E_{opt})^n / h\nu$$

Where  $n = 1/2$  for allowed transition, B is a constant and  $E_{opt}$  is direct optical band gap. For indirect transitions,

$$\alpha(\nu) = B(h\nu - E_{opt})^n / h\nu$$

Where  $n = 2$  for allowed transitions and  $E_{opt}$  is the indirect optical band gap. Using the above two equations and by plotting  $(\alpha h\nu)^{1/2}$  and  $(\alpha h\nu)^2$  as a function of photon energy  $h\nu$ , one can find the optical energy band gap ( $E_{opt}$ ) for indirect and direct transitions respectively. The respective values of  $E_{opt}$  are obtained by extrapolating to  $(\alpha h\nu)^{1/2} = 0$  for indirect transitions and  $(\alpha h\nu)^2 = 0$  for direct transitions. In order to examine the optical band gap energy for these glasses, the optical absorption spectra are also recorded in the near ultra violet region (Fig. 2). Plots drawn between  $(\alpha h\nu)^{1/2}$ ,  $(\alpha h\nu)^2$  vs  $h\nu$  are shown in Fig. 3. The optical band gap energy is obtained by extrapolating the linear region of the curve to the  $h\nu$  axis. From these plots, the optical band gap energies calculated and are given in Table 2. The optical band gap energy equation for its calculation is as follows.

$$E_{opt} = hc/\lambda$$

The optical band gap energy increases and decreases alternately with the increase of x mol % and reaches to maximum at  $x = 20$ , which shows the significance of MAE in these glasses.

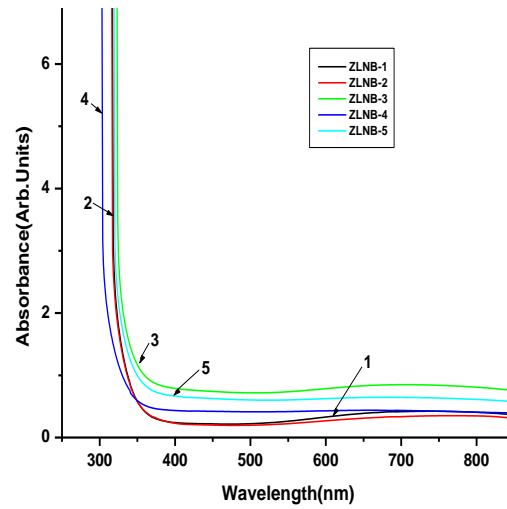


Fig. 2. Absorption edges of the optical spectra of  $\text{Cu}^{2+}$  doped ZLNB glasses.

Table 2. Absorption edge, thickness, direct, indirect optical band gaps and Urbach energies of  $\text{Cu}^{2+}$  doped ZLNB glass systems.

Glass System	Absorption edge (nm)	Thickness d (cm)	Optical band gap Energy $E_{\text{opt}}$ (eV)		Urbach energy $\Delta E$ (eV)	
			Theoretical	Experimental		
ZLNB1	318	0.140	3.906	3.893	3.856	0.024
ZLNB2	317	0.140	3.919	3.910	3.870	0.023
ZLNB3	326	0.165	3.810	3.818	3.770	0.030
ZLNB4	305	0.094	4.073	4.073	4.024	0.018
ZLNB5	320	0.153	3.882	3.866	3.830	0.025

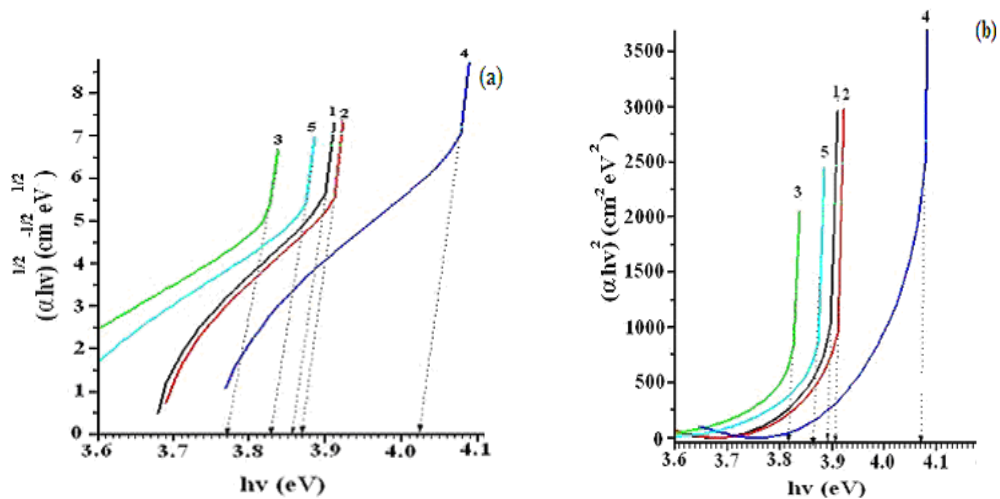


Fig. 3(a) Indirect (b) direct band gap energies of  $\text{Cu}^{2+}$  doped ZLNB glasses at room temperature.

The main feature of the absorption edge of amorphous materials is an exponential increase of the absorption coefficient  $\alpha(\nu)$  with photon energy  $h\nu$  in accordance with the empirical relation [36].

$$\alpha(\nu) = \alpha_0 \exp(h\nu / \Delta E)$$

Where  $\alpha_0$  is a constant,  $\Delta E$  is the Urbach energy which indicates the width of the band tails of the localized states and  $\nu$  is the frequency of the radiation. Therefore, Urbach energy can be considered as a measure of disorder in amorphous and crystalline materials [37–39]. The nature of disorder can be different in crystalline and amorphous solids. The disorder can be both static and dynamic in crystalline materials. Dynamic disorder arises due to electron–phonon coupling in crystalline solids. In amorphous solids, the static atomic structural disorder dominates and can be due to presence of defects like dangling bonds or non-bridging oxygen's in glasses [40]. The higher the concentration of NBOs in the glass network, the smaller is the optical energy gap and the greater are the Urbach energy values in borate glasses [41]. The excitation levels at the absorption edges are determined by the random electric fields due to either the lack of long range order or the presence of defects [42]. Urbach energies ( $\Delta E$ ) are calculated by taking the reciprocals of the slopes of linear portion in the lower photon energy regions of these curves (Fig. 4) and are listed in Table 2. The Urbach energy decreases and increases alternately with the increase of  $\text{Li}_2\text{O}$  content (Fig. 5), which shows MAE. It also shows the structural disorder of the system, where the optical band gap energy is minimum, Urbach energy is maximum and vice-versa. Smaller is the value of Urbach energy, greater is the structural stability of the glass system. It is observed that the Urbach energy is minimum at  $x = 20$  mol%.

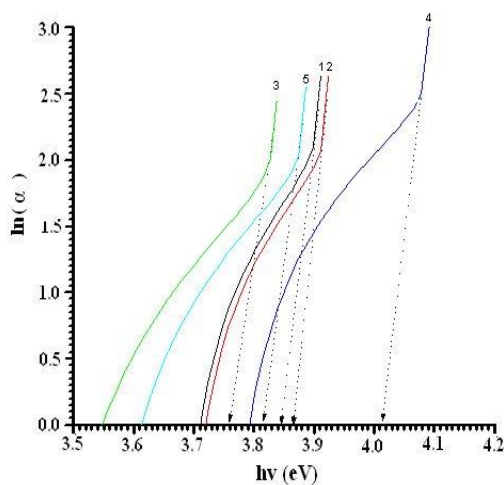


Fig. 4. Urbach energy plots of  $\text{Cu}^{2+}$  doped ZLNB glasses.

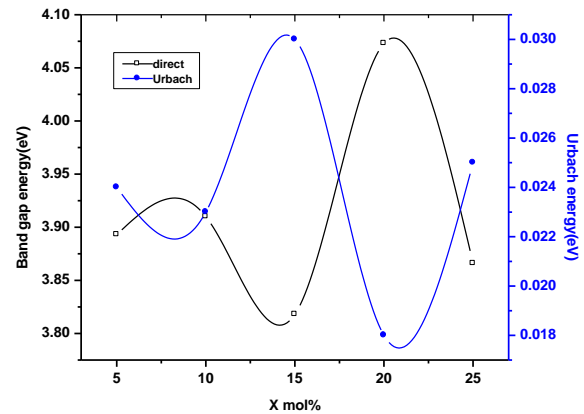


Fig. 5. Compositional dependence of band gap energy and Urbach energy of  $\text{Cu}^{2+}$  doped ZLNB glasses.

### 3.3. FT-IR studies

The experimental FT-IR spectra of the  $\text{Cu}^{2+}$  doped ( $19.9 \text{ ZnO} + x \text{ Li}_2\text{O} + (30-x) \text{ Na}_2\text{O} + 50 \text{ B}_2\text{O}_3$ , ( $5 \leq x \leq 25$ )) glasses are presented in Fig. 6. The obtained absorption bands and their assignments are summarized in Table 3. In general, the FT-IR analysis of the studied borate glasses shows four distinct frequency regions. Two regions, from  $1200$  to  $1600 \text{ cm}^{-1}$  and from  $800$  to  $1200 \text{ cm}^{-1}$ , are assigned to the stretching vibrations of both triangular  $\text{BO}_3$  and tetrahedral  $\text{BO}_4$  borate units, respectively. Deformation modes of both types of units are active between  $600$  and  $800 \text{ cm}^{-1}$  [43]. Absorption bands in the region  $400 - 550 \text{ cm}^{-1}$  are due to  $\text{ZnO}$  tetrahedron in glasses [44]. The systematic changes in the infrared spectra of these glasses are mainly observed around  $700$ ,  $1000$  and  $1400 \text{ cm}^{-1}$ . The increase of alkali oxide up to  $25 \text{ mol}\%$  leads to more number of  $\text{BO}_4$  groups, which resulting a closely packed and strongly bonded structural glass network with less number of network BOs [45]. The B-O stretching vibration of  $\text{BO}_3$  is assigned around  $1600 \text{ cm}^{-1}$ . The absorption bands around  $715 \text{ cm}^{-1}$  has been assigned to B-O-B bending vibrations, which exhibit shift towards lower wave number up to  $x = 15$  and then to higher and lower wave numbers with the increase of  $\text{Li}_2\text{O}$  content, which shows MAE. The absorption bands around  $862$  and  $884$ ,  $935 - 960$  and  $1005 - 1026 \text{ cm}^{-1}$  are assigned to symmetric stretching vibrations of B-O bonds in  $\text{BO}_4$  units, which exhibits shift towards higher wave number and then to lower wave number up to  $x = 15$  and then to higher and lower wave number with the increase of  $x \text{ mol}\%$ . The bands at  $862$  and  $884$  are attributed to non-bridging oxygen's which disappears with the increase of  $\text{Li}_2\text{O}$  content. It is observed that the alkali oxide modifies the structure by converting  $\text{BO}_3$  groups into  $\text{BO}_4$  groups. The absorption bands around  $900 - 1300 \text{ cm}^{-1}$  is assigned to characteristic zinc borate vibrations. Bands observed in the region  $1335 - 1495 \text{ cm}^{-1}$  are assigned to symmetric stretching vibrations of B-O bonds in  $\text{BO}_3$  Units. The band at  $1606 \text{ cm}^{-1}$  is assigned to asymmetric stretching vibrations of B-O bonds in  $\text{BO}_3$  units, which shifts

alternately with  $x$  mol%. The absorption band at  $457 \text{ cm}^{-1}$  is assigned to characteristic vibration of Li cation which

shifts towards lower to higher wave number and then to lower wave number with the increase of  $x$  %.

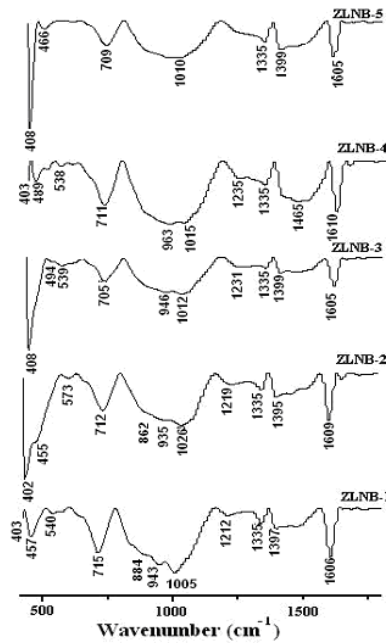


Fig. 6. FT-IR spectra of  $\text{Cu}^{2+}$  doped ZLNB glasses.

Table 3. Assignment of FT-IR bands in  $\text{Cu}^{2+}$  doped ZLNB glass systems.

Assignment	ZLNB1	ZLNB2	ZLNB3	ZLNB4	ZLNB5
	(bands in units of $\text{cm}^{-1}$ )				
Lithium Cation vibrations	457	455	494	489	466
B-O-B Bending vibrations	715	712	705	711	709
Vibrations of NBOs	884	862	----	----	----
B-O symmetric stretching	943	935	946	963	960
Vibrations of $\text{BO}_4$ units	1005	1026	1012	1015	1010
B-O stretching vibrations of trigonal $\text{BO}_3$ units of boroxyl rings	1212 1335 1397	1219 1335 1395	1231 1335 1399	1235 1335 1402	---- 1335 1399
Vibrations of NBOs In $\text{BO}_3$ units	-----	-----	-----	1465	-----
B-O asymmetric stretching vibrations of $\text{BO}_3$ units	1606	1609	1605	1610	1609

#### 4. Conclusions

From the spectral studies on  $\text{Cu}^{2+}$  doped  $19.9 \text{ ZnO} + x \text{ Li}_2\text{O} + (30-x) \text{ Na}_2\text{O} + 50 \text{ B}_2\text{O}_3$  ( $5 \leq x \leq 25$ ) glasses the following conclusions are drawn:

(i) XRD patterns confirm the amorphous nature of all the systems.

(ii) From ultraviolet absorption edges the optical band gap energies and urbach energies are evaluated. Which also confirm the structural variations with the composition of  $x$  mol%, shows MAE.

(iii) FT-IR profiles have been used to understand the bonding nature of these glasses. Strongly bonded and stable structure is observed at  $x = 20\text{mol}\%$ .

### Acknowledgements

One of the authors RVSSN would like to thank the University Grants Commission, Government of India, New Delhi for sanctioning the Major Research Project No. F. 37-2/2009 (SR) to carry out the present research work. One of the authors (T. Raghavendra Rao (F.ETFAPNA024)) is thankful to the UGC-SERO, Hyderabad, for permitting him to pursue Ph.D. programme as FDP scholar under XI plan.

### References

- [1] Xiang Peng, Feng Song, Shibin Jiang, N. Peyghambarian, Makoto K. Gonokami, Lei Xu, Appl. Phys. Lett. **82**, 10 (2003).
- [2] D. Xun, J. Yang, S. Xu, N. Dai, L. Wen, L. Hu, Z. Jiang, Chin. Phys. Lett. **20**, 130 (2003).
- [3] M. F. Churbanov, G. E. Snopatin, E. V. Zorin, S. V. Smetanin, E. M. Dianov, V. G. Plotnichenko, V. V. Koltashev, E. B. Kryukova, I. A. Grishin, G. G. \ Butsin, J. Optoelectron. Adv. Mater. **7**, 1765 (2005).
- [4] J. Pisarski, W. A. Pisarski, J. Optoelectron. Adv. Mater. **7**, 2667 (2005).
- [5] H. Kenmotsu, T. Hattori, S. Nishiyama, K. Fukushima, J. Phys. Chem. Solids **60**, 1461 (1999).
- [6] L. Zhou, H. Lin, W. Chen L. Luo, J. Phy. Chem. Solids **69**, 2499 (2008).
- [7] S. G. Lu, K. W. Kwok, H. L. W. Chan, C. L. Choy, Mater. Sci. Eng. B **99**, 491 (2003).
- [8] D. W. Kim, D. G. Lee, K. S. Hong, Mater. Res. Bull. **36**, 585 (2001).
- [9] Y. C. Lee, W. H. Lee, F. S. Shieu, Jpn. J. Appl. Phys. **41**, 6049 (2002).
- [10] R. M. Hakim, D. R. Uhlman, Phys. Chem. Glasses **8**, 174 (1967).
- [11] J. O. Isard, J. Non-Cryst. Solids **1**, 235 (1969).
- [12] D. E. Day, J. Non-Cryst. Solids **21**, 343 (1979).
- [13] P. Maass, A. Bunde, M. D. Ingram, Phys. Rev. Lett. **68**, 3064 (1992).
- [14] M. D. Ingram, Glastechn. Ber. Glass Sci. Technol. **67**, 151 (1994).
- [15] G. N. Greaves, K. L. Ngai, Phys. Rev. B **52**, 6358 (1995).
- [16] J. Swenson, A. Matic, C. Karlsson, L. Borjesson, C. Meneghini, W. S. Howells, Phys. Rev. B **63**, 132202 (2001).
- [17] J. Swenson, S. Adams, Phys. Rev. Lett. **90**, 155507 (2003).
- [18] A. Bunde, M. D. Ingram, S. Russ, Phys. Chem. Chem. Phys. **6**, 3663 (2004).
- [19] A. Faivre, D. Viviani, J. Phalippou, Solid State Ion **176**, 325 (2005).
- [20] R. P. Sreekanth Chakradhar, K. P. Ramesh, J. L. Rao, J. Ramakrishna, J. Phys. Condens. Matter **15**, 1469 (2003).
- [21] R. P. Sreekanth Chakradhar, B. Yasoda, J. Lakshmana Rao, N. O. Gopal, J. Non-Cryst. Solids **352**, 3864 (2006).
- [22] J. Krogh-Moe, Phys. Chem. Glasses **6**, 46 (1966).
- [23] R. L. Mozziand, B. E. Warren, J. Appl. Cryst. **3**, 251 (1970).
- [24] G. Giridhar, M. Rangacharyulu, R. V. S. S. N. Ravikumar, P. Sambasiva Rao, Optoelectron. Adv. Mater. – Rapid Commun. **2**, 433 (2008).
- [25] G. Giridhar, M. Rangacharyulu, R. V. S. S. N. Ravikumar, P. Sambasiva Rao, J. Mater. Sci. Technol. **25**, 531 (2009).
- [26] G. Giridhar, M. Rangacharyulu, R. V. S. S. N. Ravikumar, P. Sambasiva Rao, IOP Conf. Series: Mat. Sci. Eng. **2**, 012058 (2009).
- [27] T. Raghavendra Rao, Ch. Rama Krishna, U. S. Udayachandran Thampy, Ch. Venkata Reddy, Y. P. Reddy, P. Sambasiva Rao, R. V. S. S. N. Ravikumar, Appl. Magn. Reson. **40**, 339 (2011).
- [28] T. Raghavendra Rao, Ch. Rama Krishna, U. S. Udayachandran Thampy, Ch. Venkata Reddy, Y. P. Reddy, P. Sambasiva Rao, R. V. S. S. N. Ravikumar, Physica B **406**, 2132 (2011).
- [29] T. Raghavendra Rao, Ch. Venkata Reddy, Ch. Rama Krishna, U. S. Udayachandran Thampy, R. Ramesh Raju, P. Sambasiva Rao, R. V. S. S. N. Ravikumar, J. Non-Cryst. Solids **357**, 3373 (2011).
- [30] T. Raghavendra Rao, Ch. Venkata Reddy, Ch. Rama Krishna, D. V. Sathish, P. Sambasiva Rao, R. V. S. S. N. Ravikumar, Mater. Res. Bull. **46**, 2222 (2011).
- [31] T. Raghavendra Rao, Ch. Rama Krishna, Ch. Venkata Reddy, U. S. Udayachandran Thampy, Y. P. Reddy, P. S. Rao, R. V. S. S. N. Ravikumar, Spectrochimica Acta **79**, 1116 (2011).
- [32] G. Krishna Kumari, Sk. Muntaz Begum, Ch. Rama Krishna, D. V. Sathish, P. N. Murthy, P. S. Rao, R. V. S. S. N. Ravikumar, Mater. Res. Bull., **47**, 2646 (2012).
- [33] G. Krishna Kumari, Ch. Rama Krishna, Sk. Muntaz Begum, V. Pushpa Manjari, P. N. Murthy, R. V. S. S. N. Ravikumar, Spectrochim. Acta **A100**, 140 (2013).
- [34] H. Ticha, L. Tichy, Optoelectron. Adv. Mater– Rapid Commun. **5**, 1277 (2011).
- [35] E. A. Davis, N. F. Mott, Phil. Mag. **22**, 903 (1970).
- [36] M. A. Hassan, C. A. Hogarth, J. Mater. Sci. **23**, 2500 (1988).
- [37] F. Urbach, Phys. Rev. **92**, 1324 (1953).
- [38] D. Redfield, Phys. Rev. **130**, 916 (1963).
- [39] D. L. Dexter, Phys. Rev. Lett. **19**, 1383 (1967).
- [40] I. A. Weinstein, A. F. Zatsepin, V. S. Kortov, J. Non-Cryst. Solids **279**, 77 (2001).
- [41] R. D. Sheibani, C. A. Hogarth, J. Mater. Sci. **26**, 429 (1991).
- [42] G. Fuxi, “Optical Spectroscopic Properties of Glass”, Springer, Berlin, p.62 (1992).
- [43] M. S. Gaafar, N. S. Abd El-Aal, O. W. Gerges, G. El-Amir, J. Alloys and Compd. **475**, 535 (2009).
- [44] P. Tarte, Bull. Soc. Fr. Ceram. **58**, 13 (1963).
- [45] W. Soppe, V. Althof, H. W. Den Hartog, J. Non-Cryst. Solids **104**, 22 (1988).